Electrical Characteristics of Non-thermal Dielectric Barrier Discharge Devices with Coaxial Wire-cylinder and Wire-windings Configurations

Ahmad Zulazlan[1], Mooktzeng Lim[1], Kanesh Kumar Jayapalan[2], Kailok Lai[2], and Oihoong Chin[2]
[1]*Fuels & Combustion, Generation, TNB Research Sdn. Bhd., Malaysia.*
[2]*Plasma Technology Research Center, Physics Department, University of Malaya, Malaysia.*
mooktzeng.lim@tnbr.com.my

***Abstract*—To ensure the sustainability of fuel resources and to reduce cost from thermal processes such as combustion, a non-thermal plasma device (NTP) was proposed in this study. NTP devices have been known to reduce pollutants in flue gas and also assist in combustion. As opposed to thermal plasmas, NTPs utilize the energy to create radicals or excited species of the carrier gases that flow through the device. Before the NTP device is applied for combustion, its performance (namely, the amount of energy it consumes and generates) needs to be characterized. Thus, this study investigates the discharge characteristics of two different types of NTP configuration – dielectric barrier discharge (DBD) reactors with (a) wire-cylinder and (b) wire-windings arrangements. The power consumption and discharge power were also measured to determine their efficiency. The discharge power was determined via the Lissajous diagram, which is a plot of the charge accumulated in the discharge against the discharge voltage. The Lissajous diagram of both configurations was a parallelogram, typical of DBDs. The wire-windings arrangement required lower sustaining voltage and was generally more efficient in terms of power consumption.**

***Index Terms*—Dielectric Barrier Discharge; Electrical Characteristics; Non-Thermal Plasma.**

I. INTRODUCTION

In this research project, a non-thermal plasma (NTP) device is developed for the mitigation of pollutants in flue gas and possibly assisting in combustion [1]. As opposed to thermal plasmas, NTPs utilize the energy to create radicals or excited species of the carrier gases that flow through the device [2]. If the carrier gas is air, it undergoes electron impact with the electron avalanche or streamers. This then produces radicals or oxygen molecules that are in an excited state which has higher energy levels than their ground state [2, 3]. These radicals have been known to accelerate heat release in combustion reactions and augment flame characteristics [4-7]. In addition, non-thermal plasma devices have been used to mitigate pollutants [8-10]. The ability to burn leaner mixtures allows the possibility of operating combustion processes at lower fuel flow rates without the disadvantages of unstable flames or operation. This would also mean that with the introduction of more reactive air via NTP devices, combustion processes can operate on lower fuel consumption and thus reduce operating costs [3].

Before the NTP device is applied for combustion, its performance (namely, the amount of energy it consumes and generates) needs to be characterized. Thus, this study investigates the discharge characteristics of two different types of NTP configuration. The power consumption and discharge power were also measured to determine their efficiencies.

II. METHODOLOGY

Two dielectric barrier discharge (DBD) reactors of different configurations: (a) wire-cylinder with annular gap arrangement, and (b) wire-windings arrangement, were used to determine the power consumption (the power consumed from the mains power supply) and the discharge power (the amount of power dissipated in the DBD discharge). The electrode arrangements are shown in Figure 1. In the case of the wire-cylinder setup, nitrogen:oxygen gas mixture in the ratio of 15:4 (close to composition in air) was flowed through the annular gap, the total gas flow rate was 19 l/min.

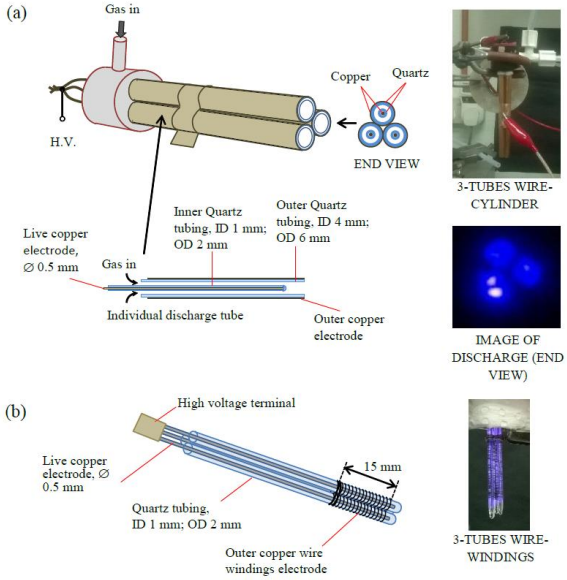

Figure 1: Schematic of the DBD reactors: (a) wire-cylinder with annular air gap for gas flow configuration, and (b) wire-windings configuration.

The reactors were powered by the PVM500 Plasma Resonant Driver (Figure 2) that had to be frequency tuned to match the capacitive load. The working frequency was 25.6 ± 0.1 kHz. The discharge voltage was measured by the Tektronix P6015A high voltage probe, while the current was monitored by the Pearson 4100 current transformer and the data was recorded by the Tektronix TDS2024C 200MHz, 2 GS/s oscilloscope. The power consumption was determined via the power monitor EM561 that measures the average power drawn from the mains power supply (with accuracy 1% ± 5 digits). The discharge power was determined by measuring the voltage across a series 0.1 μF capacitor inserted between to the outer electrode and ground point, from which the charge transported in the discharge can then be calculated ($Q = CV$). A plot of the charge against the discharge voltage gives a Lissajous curve, and the area under the curve will yield the energy dissipated in the discharge. Multiplying this energy with the frequency of the applied voltage gives the discharge power per cycle [11].

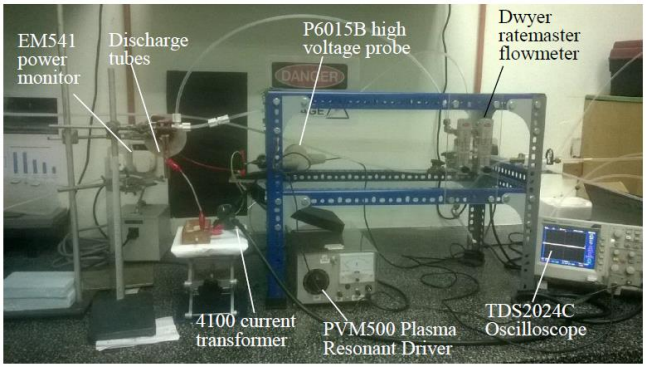

Figure 2: Experimental set-up.

III. Results And Discussion

Representative voltage and current waveforms for the DBD reactors at various discharge voltages are shown in Figure 3. The power source can sustain the discharges up to maximum 13.0 kV, 0.05 A for the wire-cylinder setup; and 9.9 kV, 0.04 A for the wire-windings configuration. The values stated in this paper are the peak-to-peak values, unless otherwise indicated. The current leads the voltage by 90° for these capacitive arrangements. The peak current increases with increasing (applied) voltage, the filamentary discharges become more intense (larger amplitude and increase in number of spikes in the current waveforms). The filamentary discharges occurred mostly at the first and third quadrants of the voltage signals.

Figure 4 shows the Lissajous diagram for the respective DBD reactors at various discharge voltages. The parallelogram shown is widely reported in literature [12-13]. The efficiency is defined as the ratio of the dissipated discharge power, P_o and the average power consumed by the high voltage generator, P_{in}. The total capacitance of each reactor deduced from the Lissajous diagrams are 10.5 and 5.2 pF for the respective wire-cylinder and wire-windings arrangements. From the cross sections in Figure 5, the capacitances per unit length can be deduced from:

Wire-cylinder:
$$\frac{L}{C_{T(W-C)}} = \frac{\ln(r_1/r_0)}{2\pi\varepsilon_0\varepsilon_{rq}} + \frac{\ln(r_2/r_1)}{2\pi\varepsilon_0} + \frac{\ln(r_3/r_2)}{2\pi\varepsilon_0\varepsilon_{rq}} \quad (1)$$

Wire-windings:
$$\frac{L}{C_{T(W-W)}} = \frac{\ln(r_1/r_0)}{2\pi\varepsilon_0\varepsilon_{rq}} \quad (2)$$

where ε_0 = permittivity in free space (8.854×10^{-12} F/m), ε_{rq} = dielectric constant for quartz (3.8) [14], $r_0 = 0.5$, $r_1 = 1.5$, $r_2 = 2.0$, and $r_3 = 3.0$ mm. The computed capacitances are 19.5 pF and 8.7 pF which is an over-estimate, but the order of magnitude is comparable to the measured values above. The wire-cylinder DBD reactor has larger surface area for discharge (length is longer) and needs a higher voltage to be sustained as there is an annular air gap of 1 mm with gas flow when the current is ≥0.01 A as shown in Figure 6. The wire-windings configuration has smaller surface area (as the discharge length is approximately 20% of the wire-cylinder arrangement) and the separation between the inner and outer electrodes is smaller with no air-gap between them.

The power consumption and efficiency of both the reactors operated at different voltages and currents are compared in Figure 7. At fixed discharge voltages, the wire-windings DBD reactor allowed more efficient utilization of the energy resulting in more charges transferred in the DBD. At fixed discharge currents, the wire-windings configuration produced higher efficiency except at currents above 0.025 A where both reactors showed almost the same efficiency (within experimental uncertainty). This could be due to the profuse filamentary discharges filling up the entire length of the air-gap in the wire-cylinder reactor – this can be seen in the current waveforms in Figure 3 whereby the current spikes were appearing more densely at voltage above 10.1 kV.

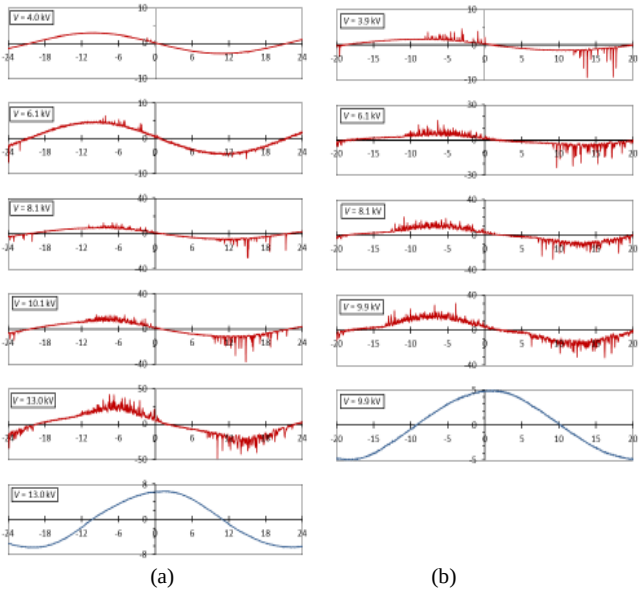

Figure 3: Current (red curve) and voltage (blue curve at the bottom) waveforms at different discharge voltages for the DBD reactors: (a) wire-cylinder and (b) wire-windings configurations.

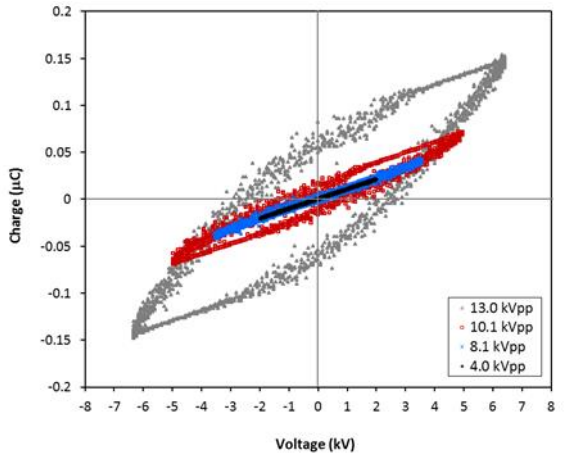

(a)

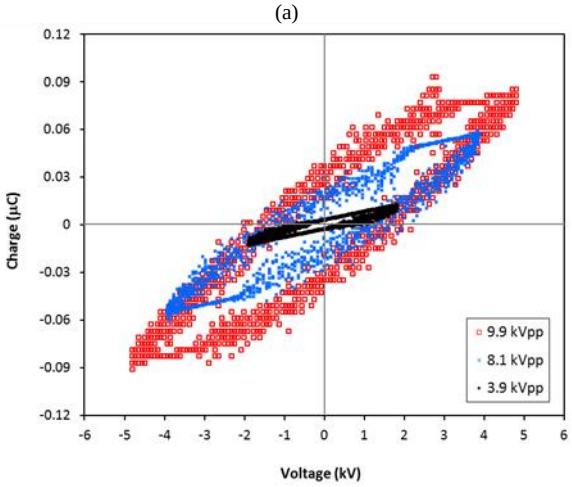

(b)

Figure 4: Lissajous diagram for the respective DBD reactors: (a) wire-cylinder, and (b) wire-windings configurations at various discharge voltages.

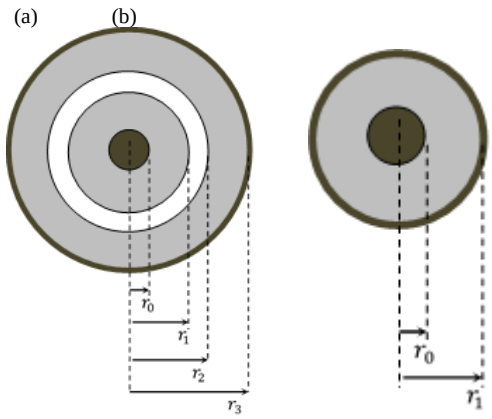

Figure 5: Cross sections of the: (a) wire-cylinder, and (b) wire-windings configurations for determination of capacitances. The outer windings in (b) are assumed to be a cylindrical conductor.

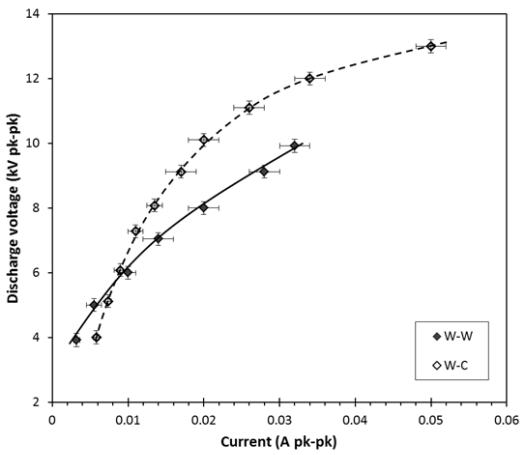

Figure 6: Relationship between the discharge voltage and current for the wire-cylinder (W-C) and wire-windings (W-W) configurations.

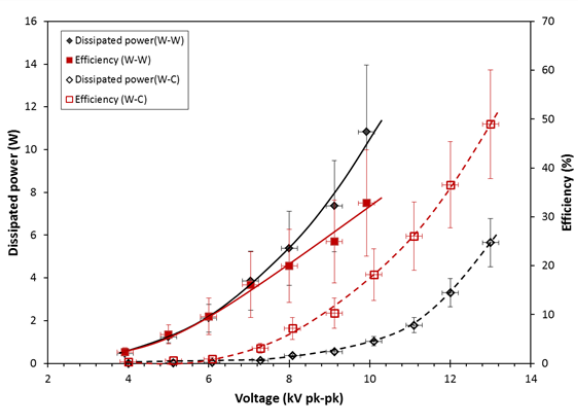

(a)

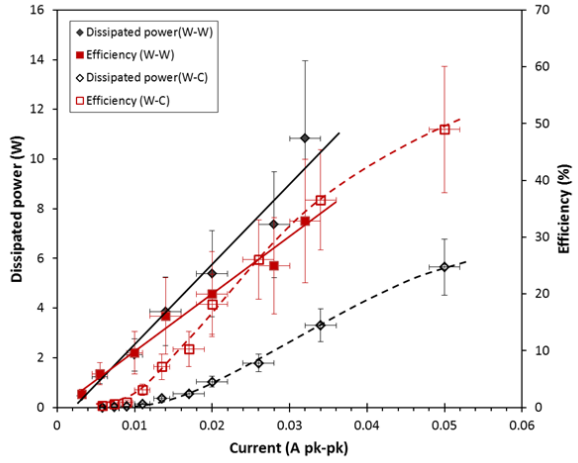

(b)

Figure 7: Efficiency and power dissipated in the respective DBD reactors, wire-cylinder (W-C) and wire-windings (W-W) configurations at different discharge (a) voltages and (b) currents.

IV. CONCLUSION

This study compares the electrical characteristics of two DBD reactors (wire-cylinder with gap and wire-windings configurations) that are being considered for used in assisting combustion related processes. Both Lissajous curves are typical of DBD. In general, the wire-windings configuration required lower voltage to sustain and displayed higher efficiency. However, this configuration did not incorporate any gas flow and the discharge was observed to occur along the outer surface of the quartz tube in direct contact with the wire winding electrode. The presented work is a preliminary study and detailed parametric study is in progress.

ACKNOWLEDGMENT

The authors would like to thank TNBR for the funding of this research (TNBR/SF0195) and MOHE for the support of FRGS Grant No. FP017-2013A. The authors would also like to acknowledge the assistance from all of those involved in the project.

REFERENCES

[1] E. I. Karpenko, V. E. Messerle, and A. B. Ustimenko, "Plasma-aided solid fuel combustion," *P. Combust. Inst.*, vol. 31, pp. 3353–3360, 2007.

[2] M. Sjöberg, Yu. V. Serdyuk, S. M. Gubanski, and M. Å. S. Leijon. "Experimental study and numerical modelling of a dielectric barrier discharge in hybrid air–dielectric insulation," *J. Electrostat.*, vol. 59, pp. 87–113, 2003.

[3] A. Starikovskiy, and N. Aleksandrov, "Plasma-assisted ignition and combustion," *Prog. Energy Combust. Sci.*, vol. 39, pp. 61–110, 2013.

[4] T. Ombrello, S. H. Won, Y. Ju, and S. Williams, "Flame propagation enhancement by plasma excitation of oxygen. Part II: Effects of $O_2(a^1\Delta_g)$," *Combust. Flame*, vol. 157, pp. 1916–1928, 2010.

[5] T. Ombrello, S. H. Won, Y. Ju, and S. Williams, "Flame propagation enhancement by plasma excitation of oxygen. Part I: Effects of O_3," *Combust. Flame*, vol. 157, pp. 1906–1915, 2010.

[6] B. F. W. Vermeltfoort, "Experimental investigation of plasma assisted combustion using a low swirl burner," *MSc. Thesis*, WVT 2010.10, Eindhoven University of Technology, Eindhoven, Netherlands, 2010.

[7] W. Sun, M. Uddi, T. Ombrello, S. H. Won, C. Carter, and Y. Ju, " Effects of non-equilibrium plasma discharge on counterflow diffusion flame extinction," *P. Combust. Inst.*, vol. 33, pp. 3211–3218, 2011.

[8] U. Kogelschatz, B. Eliasson, and W. Egli, "Dielectric-Barrier Discharges. Principle and Applications," *J. Phys. IV*, vol 7. pp. C4-47–C4-66, 1997.

[9] A. A., Assadi, A. Bouzaza, M. Lemasle, and D. Wolbert, "Removal of trimethylamine and isovaleric acid from gas streams in a continuous flow surface discharge plasma reactor," *Chem. Eng. Res. Des.*, vol. 93, pp. 640-651, 2015.

[10] A. A., Assadi, A. Bouzaza, and D. Wolbert, "Study of synergetic effect by surface discharge plasma/TiO2 combination for indoor air treatment: Sequential and continuous configurations at pilot scale," *J. Photochem. Photobiol. A Chem.*, vol. 310, pp. 148–154, 2015.

[11] T. C. Manley, "The electric characteristics of the ozonator discharge". *J. Electrochem. Soc.*, vol. 84, no. 1, pp. 83–96, 1943.

[12] Y. P. Hao, J. Y. Chen, L. Yang, and X. L. Wang, "Lissajous figures of glow and filamentary dielectric barrier discharges under high frequency voltage at atmospheric pressure in helium", in *Proceedings of 9th International Conference on Properties and Applications of Dielectric Materials*, Harbin, China, 2009, pp. 590-593.

[13] I. Biganzoli, R. Barni, A. Gurioli, R. Pertile, and C. Riccardi. "Experimental investigation of Lissajous figure shapes in planar and surface dielectric barrier discharges", *J. Phys. Conf. Ser.*, vol. 550, pp. 012-039, 2014.

[14] Tables of Physical & Chemical Constants (16th edition). 2005. 2.6.5 Dielectric properties of materials. Kaye & Laby Online. Version 1.0. www.kayelaby.npl.co.uk